

Crystal Structures and Electrical Conductivities of $\text{TXC}_n\text{-TTF}$ ($\text{X}=\text{Sulfur, Selenium, Tellurium}$; $n=2,3$) · TCNQ Charge-Transfer Complexes

Kenichi IMAEDA,* Takehiko MORI, Chikako NAKANO, Hiroo INOKUCHI,
Naoko IWASAWA,[†] and Gunzi SAITO^{†,††}

Institute for Molecular Science, Myodaiji, Okazaki 444

[†] Institute for Solid State Physics, The University of Tokyo,

Roppongi, Minato-ku, Tokyo 106

(Received October 25, 1990)

The crystal structures and the electrical conductivities have been studied for tetrakis(alkylchalcogeno)tetrathiafulvalene ($\text{TXC}_n\text{-TTF}$ ($\text{X}=\text{sulfur, selenium, tellurium}$; $n=2,3$)) complexes with tetracyanoquinodimethane (TCNQ). All the complexes with a composition of 1 : 1 had the same crystal system (triclinic) and the same space group ($P1$). The donor and acceptor molecules were alternately stacked in their crystals. ($\text{TSeC}_2\text{-TTF}$)TCNQ was obtained as plate and needle crystals. The molecular structure of $\text{TSeC}_2\text{-TTF}$ and the overlapping mode between $\text{TSeC}_2\text{-TTF}$ and TCNQ molecules of the two complexes were subtly different. All the complexes were semiconductors because of their mixed-stack structures. ($\text{TTeC}_2\text{-TTF}$)TCNQ showed the lowest resistivity ($5\ \Omega\ \text{cm}$ at room temperature). Its good conductivity was brought about by the effective degree of charge-transfer and the favorable overlap between $\text{TTeC}_2\text{-TTF}$ and TCNQ molecules. An overall discussion on the structural and physical properties of a series of TCNQ complexes with $\text{TXC}_n\text{-TTF}$ ($\text{X}=\text{sulfur, selenium, tellurium}$; $n=1,2,3$) is presented.

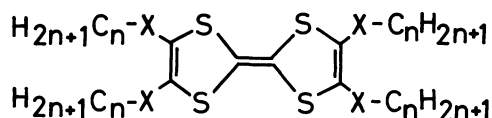
Tetrakis(alkylchalcogeno)tetrathiafulvalene ($\text{TXC}_n\text{-TTF}$) has exhibited novel electronic properties as a consequence of the intermolecular interactions between the tetrachalcogeno-TTF conjugated π systems and the alkyl side chains. $\text{TTC}_n\text{-TTF}$ compounds with long alkyl chains had relatively low resistivities because of a reduction of the interplanar distances between the TTF skeletons through the van der Waals interactions of the alkyl side chains between molecules. This was termed "a molecular fastener effect".^{1–4)} This finding was significant since high conductivities in single-component organic solids are produced not by an external pressure but by an internal pressure derived from attractive forces between attached organic functional groups. $\text{TTeC}_1\text{-TTF}$ is a new organic semiconductor with high electrical conductivity and high carrier mobility, which does not belong to the category of molecular fasteners. The unusual properties of $\text{TTeC}_1\text{-TTF}$ are caused by a formation of regular Te chains through quasi-covalent Te–Te interatomic contacts between neighboring $\text{TTeC}_1\text{-TTF}$ stacks.⁵⁾

$\text{TXC}_n\text{-TTF}$ compounds are also attractive donors used in the formation of charge-transfer (CT) complexes.^{6–9)} $\text{TXC}_1\text{-TTF}$ complexes with various acceptors have been actively investigated and a metallic conductivity has been found in ($\text{TTC}_1\text{-TTF}$)(I_3)_{0.823}.^{10–13)} $\text{TXC}_n\text{-TTF}$ compounds with long alkyl side chains may form highly conductive CT complexes since they are expected to generate charge carriers in addition to their fastener effect. The present system allows us to systematically study how the chain length of alkyl groups and the variation of chalcogen atoms affect the physical properties of the complexes.

Various ($\text{TXC}_1\text{-TTF}$)–TCNQ complexes have been previously studied: the crystal structures and the physical properties of ($\text{TTC}_1\text{-TTF}$)TCNQ and ($\text{TTC}_1\text{-TTF}$)₂TCNQ were reported by Mori et al.¹⁴⁾ and those of ($\text{TSeC}_1\text{-TTF}$)TCNQ and ($\text{TTeC}_1\text{-TTF}$)TCNQ were reported by Iwasawa et al.^{9,15,16)} In this work, we prepared single crystals of $\text{TXC}_n\text{-TTF}$ ($\text{X}=\text{S, Se, Te}$; $n=2,3$) complexes with TCNQ. We present the experimental results of their crystal structure determinations and electrical conductivity measurements. The correlation between the structure and the conductivity is discussed on the basis of the degree of charge-transfer (ionicity) and the molecular overlap between the donor and the acceptor.

Experimental

Black single crystals of $\text{TXC}_n\text{-TTF}$ ($\text{X}=\text{S, Se, Te}$; $n=2,3$) · TCNQ were prepared by mixing hot CH_3CN solutions of each component and then keeping the solutions cool in a refrigerator (5°C) or a freezer (-20°C) for several days. ($\text{TTC}_2\text{-TTF}$)TCNQ, ($\text{TSeC}_3\text{-TTF}$)TCNQ, ($\text{TTeC}_2\text{-TTF}$)TCNQ, and ($\text{TTeC}_3\text{-TTF}$)TCNQ crystallized in needles, while ($\text{TTC}_3\text{-TTF}$)TCNQ crystallized in plates. In the case of ($\text{TSeC}_2\text{-TTF}$)TCNQ, two kinds of crystals were obtained depending on



$\text{X}=\text{S}$: $\text{TTC}_n\text{-TTF}$
 Se : $\text{TSeC}_n\text{-TTF}$
 Te : $\text{TTeC}_n\text{-TTF}$

Scheme 1.

^{††} Present address: Department of Chemistry, Faculty of Science, Kyoto University, Sakyo-ku, Kyoto 606.

Table 1. Crystallographic Data of (TXC_n-TTF)TCNQ

	(TTC ₂ -TTF)TCNQ	(TTC ₃ -TTF)TCNQ	(TSeC ₂ -TTF)TCNQ	(TSeC ₃ -TTF)TCNQ	(TTeC ₂ -TTF)TCNQ	(TTeC ₃ -TTF)TCNQ
Chemical formula	C ₂₆ H ₂₄ N ₄ S ₈	C ₃₀ H ₃₂ N ₄ S ₈	C ₂₆ H ₂₄ N ₄ S ₄ Se ₄	C ₃₀ H ₃₂ N ₄ S ₄ Se ₄	C ₂₆ H ₂₄ N ₄ S ₄ Te ₄	C ₃₀ H ₃₂ N ₄ S ₄ Te ₄
FW	649.02	705.13	836.60	892.71	1031.16	1087.27
Crystal shape	Needle	Plate	Plate	Needle	Needle	Needle
Crystal system	Triclinic	Triclinic	Triclinic	Triclinic	Triclinic	Triclinic
Space group	$P\bar{1}$	$P\bar{1}$	$P\bar{1}$	$P\bar{1}$	$P\bar{1}$	$P\bar{1}$
<i>a</i> /Å	9.143(1)	9.107(1)	9.168(1)	9.140(1)	9.203(2)	10.285(2)
<i>b</i> /Å	11.374(2)	13.197(2)	11.418(1)	11.430(2)	12.918(2)	13.245(2)
<i>c</i> /Å	8.052(1)	8.168(1)	8.382(1)	8.181(1)	8.494(3)	8.467(2)
α /°	95.37(1)	98.29(2)	92.14(1)	95.29(1)	96.91(2)	81.96(2)
β /°	105.83(1)	109.19(1)	110.66(1)	105.31(1)	111.52(2)	121.48(1)
γ /°	100.93(1)	101.58(1)	100.68(1)	99.83(1)	101.88(2)	108.09(2)
<i>V</i> /Å ³	781.5(2)	884.4(3)	801.8(2)	803.7(2)	821.0(2)	934.6(4)
<i>Z</i>	1	1	1	1	1	1
<i>D_x</i> /g cm ⁻³	1.379	1.324	1.733	1.729	2.086	1.932
<i>R</i>	0.048	0.078	0.057	0.050	0.038	0.039
μ (Mo <i>K</i> α)/cm ⁻¹	5.71	5.10	48.03	47.91	37.96	33.39
(sin θ /λ) _{max}	0.7014	0.7009	0.7035	0.7035	0.7026	0.6965
No. of reflections	1205	1730	2516	2180	4074	1445

the temperature; plates formed at 5 °C and needles formed at -20 °C.

X-Ray diffraction data were collected at room temperature with a Rigaku AFC-5 automated four circle diffractometer with monochromatized Mo *K*α ($\lambda=0.71069$ Å) radiation in the range of $2\theta<60^\circ$ using a θ - 2θ scan technique. The unit cell parameters were determined by a least-squares fit of 50 reflections with $20^\circ<2\theta<30^\circ$. The crystallographic data are summarized in Table 1. The independent reflections ($|F_o|>3\sigma(|F_o|)$) were used for structure analyses. The crystal structures were solved by the Patterson method for (TTeC₃-TTF)TCNQ and the direct method using the MULTAN 78 program system¹⁷⁾ for the other complexes, and were refined by the block diagonal least-square method after an absorption correction. Anisotropic thermal parameters were adopted for non-hydrogen atoms and the hydrogen atoms were refined isotropically. The atomic scattering factors were taken from the International Tables for X-ray Crystallography.¹⁸⁾ All the calculations were carried out on a HITAC M-680H computer with the UNICS III program system.¹⁹⁾ The atomic parameters are listed in Table 2.²⁰⁾

The electrical conductivity along the long axis of the crystals, which corresponds to the *a*-axis, was measured between room temperature and 200 K with a four-probe method for (TTeC₂-TTF)TCNQ and a two-probe method for the other complexes using a gold paste as electrical contacts.

Results and Discussion

Crystal Structure. The TXC_{*n*}-TTF (*X*=S, Se, Te; *n*=2,3) complexes with TCNQ crystallized in the triclinic system and the $P\bar{1}$ space group, as listed in Table 1. (TTC₂-TTF)TCNQ and (TSeC₃-TTF)TCNQ crystals were isomorphous to the (TSeC₂-TTF)TCNQ needle-shaped crystal (abbreviated as n-(TSeC₂-TTF)TCNQ). (TTC₃-TTF)TCNQ and (TTeC₂-TTF)TCNQ crystals were isomorphous to the (TSeC₂-TTF)TCNQ plate-shaped crystal (abbreviated as p-(TSeC₂-TTF)TCNQ). The crystal structure of (TTeC₂-TTF)TCNQ was identical to that reported by Ahalon-Shalom et al.²¹⁾ Therefore, we have described the crystal structures of p-(TSeC₂-TTF)TCNQ and n-(TSeC₂-TTF)TCNQ only.

The molecular structures with atomic numbering schemes for p-(TSeC₂-TTF)TCNQ and n-(TSeC₂-TTF)TCNQ are illustrated in Figs. 1 and 2, respectively. The tetraseleno-TTF (C₆S₄Se₄) moieties in both complexes are nearly planar, in contrast to the nonplanar structure in the crystal of uncomplexed TSeC₂-TTF.²²⁾ The ethyl groups attached to Se(2) of p-(TSeC₂-TTF)TCNQ lie almost coplanar to the C₆S₄Se₄ plane. The other ethyl groups attached to Se(1) are perpendicular to the C₆S₄Se₄ plane. This configuration of the molecule is denoted as the p-form. In contrast, the four ethyl groups of n-(TSeC₂-TTF)TCNQ are perpendicular to the C₆S₄Se₄ plane. This configuration of the molecule is denoted as the n-form. The comparatively large temperature factors of the terminal carbon atoms of the ethyl groups in both complexes may be caused by large thermal vibrations. The molecular structure of TCNQ in these complexes is planar with a

Table 2. Positional Parameters ($\times 10^4$) and Equivalent Isotropic Thermal Parameters (\AA^2) of (TxC_n-TTF)TCNQ

Atom	<i>x</i>	<i>y</i>	<i>z</i>	<i>B</i> _{eq}	Atom	<i>x</i>	<i>y</i>	<i>z</i>	<i>B</i> _{eq}
(TTC ₂ -TTF)TCNQ					(TSeC ₂ -TTF)TCNQ Needle Crystal				
S1	7501(2)	-2321(2)	8709(3)	6.6	Se1	7527(1)	-2231(1)	8941(1)	5.7
S2	5586(2)	-3383(2)	4543(3)	6.4	Se2	5636(1)	-3482(1)	4718(1)	5.6
S3	9510(2)	-461(1)	7407(2)	5.2	S1	9506(2)	-397(2)	7403(3)	4.7
S4	7897(2)	-1421(1)	3700(2)	4.7	S2	7973(2)	-1442(1)	3802(3)	4.3
C1	9471(6)	-398(5)	5236(8)	4.3	C1	9487(8)	-381(6)	5269(9)	3.8
C2	7981(7)	-1762(5)	6929(8)	4.7	C2	8009(8)	-1685(6)	6.993(9)	4.2
C3	7246(6)	-2192(5)	5250(8)	4.4	C3	7321(8)	-2147(6)	5374(9)	3.9
C4	9202(9)	-2843(7)	9680(9)	7.7	C4	9373(12)	-2847(9)	9787(12)	8.2
C5	9504(9)	-3829(7)	8540(11)	12.2	C5	9587(13)	-3814(10)	8593(14)	9.3
C6	5656(8)	-4132(6)	2508(9)	7.8	C6	5642(11)	-4070(9)	2489(12)	8.7
C7	6856(9)	-4795(7)	2667(12)	9.7	C7	6864(13)	-4770(10)	2476(16)	10.6
CC1	6184(6)	847(5)	6263(8)	4.7	CC1	6157(8)	865(7)	6205(9)	4.6
CC2	6002(6)	869(5)	4427(8)	4.4	CC2	6002(8)	835(6)	4444(9)	4.1
CC3	4754(7)	-19(5)	3207(8)	4.8	CC3	4791(9)	-62(7)	3246(9)	4.7
CC4	6965(7)	1711(5)	3866(8)	4.8	CC4	6965(8)	1658(7)	3829(10)	4.9
CC5	8203(7)	2609(5)	5062(8)	5.5	CC5	8160(9)	2570(7)	4980(11)	5.5
CC6	6810(7)	1762(5)	2058(9)	6.2	CC6	6806(9)	1661(8)	2038(10)	6.1
N1	9181(7)	3327(5)	6038(8)	7.7	N1	9111(8)	3281(7)	5918(10)	7.5
N2	6679(8)	1799(6)	633(8)	9.4	N2	6698(10)	1674(8)	641(10)	9.1
(TTC ₃ -TTF)TCNQ					(TSeC ₃ -TTF)TCNQ				
S1	8771(3)	1963(2)	9721(3)	7.1	Se1	7178(1)	-2041(1)	8234(1)	6.3
S2	7877(3)	3041(2)	6222(3)	7.5	Se2	5159(1)	-3166(1)	3657(1)	6.4
S3	9706(2)	366(2)	7563(3)	6.3	S1	9420(2)	-403(2)	7174(3)	4.9
S4	8889(2)	1287(2)	4416(3)	6.0	S2	7788(2)	-1313(2)	3436(3)	4.7
C1	9713(8)	338(5)	5412(9)	5.5	C1	9415(8)	-368(5)	5127(10)	4.4
C2	9010(8)	1504(5)	7723(9)	5.6	C2	7789(8)	-1558(5)	6472(10)	4.2
C3	8640(8)	1936(5)	6315(9)	5.5	C3	7056(8)	-1985(5)	4796(10)	4.2
C4	10835(11)	2534(7)	11164(10)	9.7	C4	9236(10)	-2310(6)	9631(10)	5.8
C5	11617(13)	3525(12)	10730(13)	19.1	C5	9646(10)	-3238(7)	8818(11)	5.6
C6	12835(22)	4187(12)	11747(18)	21.5	C6	8482(12)	-4317(7)	8531(13)	7.5
C7	7877(13)	3325(7)	4105(12)	10.8	C7	6003(12)	-4155(7)	2447(13)	8.5
C8	7424(16)	4221(8)	3761(14)	14.2	C8	6899(15)	-4733(9)	3573(17)	10.8
C9	7264(17)	4448(8)	2027(15)	14.8	C9	7430(15)	-5585(8)	2610(16)	10.1
CC1	5155(8)	-68(5)	6747(8)	5.1	CC1	6268(8)	828(5)	6325(9)	3.9
CC2	4549(7)	762(5)	5978(8)	4.8	CC2	6054(7)	747(5)	4569(9)	3.8
CC3	4427(7)	788(5)	4191(8)	5.0	CC3	4753(8)	-113(5)	3237(9)	4.0
CC4	4114(8)	1504(5)	6958(8)	5.5	CC4	7097(9)	1462(5)	4098(9)	4.3
CC5	4193(8)	1493(5)	8753(9)	6.2	CC5	8377(9)	2340(6)	5372(10)	4.9
CC6	3528(9)	2341(5)	6301(9)	6.4	CC6	6938(9)	1388(6)	2341(11)	5.3
N1	4528(8)	1467(5)	10168(8)	8.3	N1	9410(8)	3027(6)	6370(9)	7.2
N2	3053(8)	3019(5)	5761(9)	8.8	N2	6810(9)	1332(6)	951(9)	7.5
(TSeC ₂ -TTF)TCNQ Plate Crystal					(TTeC ₂ -TTF)TCNQ				
Se1	8557(1)	2166(1)	9394(1)	5.7	Te1 ^{a)}	83735(3)	21556(2)	95134(3)	4.1
Se2	7802(1)	3657(1)	5759(1)	5.7	Te2 ^{a)}	77926(3)	38785(2)	57381(3)	3.7
S1	9605(2)	345(1)	7392(2)	4.8	S1	9505(1)	302(1)	7332(1)	3.8
S2	8897(2)	1537(1)	4252(2)	4.7	S2	8946(1)	1570(1)	4286(1)	3.7
C1	9703(6)	392(4)	5363(6)	4.2	C1	9679(4)	392(3)	5347(5)	3.4
C2	8881(6)	1657(4)	7384(6)	4.1	C2	8777(4)	1614(3)	7327(4)	3.1
C3	8567(6)	2210(4)	5971(6)	4.0	C3	8530(4)	2216(3)	5943(4)	3.0
C4	10790(9)	2762(7)	10824(8)	7.8	C4	10802(6)	2840(5)	10834(6)	6.1
C5	11649(9)	3744(7)	10241(10)	8.7	C5	11602(6)	3767(5)	10048(8)	6.7
C6	8001(12)	4117(8)	3428(14)	12.5	C6	7667(7)	4076(5)	3186(6)	6.2
C7	6666(15)	3704(12)	2494(17)	19.0	C7	6117(9)	3921(8)	2043(8)	10.8
CC1	5062(6)	-131(5)	6681(6)	4.2	CC1	4995(4)	-169(3)	6635(4)	3.4
CC2	4461(5)	839(4)	5822(6)	4.0	CC2	4395(4)	807(3)	5788(4)	3.3
CC3	4424(6)	932(5)	4102(6)	4.3	CC3	4435(4)	935(3)	4115(5)	3.4
CC4	3919(6)	1656(5)	6611(6)	4.5	CC4	3798(4)	1597(3)	6561(5)	3.7
CC5	3906(7)	1550(5)	8300(7)	5.5	CC5	3747(5)	1474(4)	8221(5)	4.4
CC6	3352(7)	2649(5)	5797(7)	5.9	CC6	3236(5)	2599(4)	5764(6)	4.5
N1	3879(7)	1455(5)	9641(6)	7.9	N1	3691(6)	1359(4)	9539(5)	6.5
N2	2892(8)	3430(5)	5140(7)	8.5	N2	2777(6)	3389(4)	5098(6)	6.3

Table 2. (Continued)

Atom	x	y	z	B_{eq}	Atom	x	y	z	B_{eq}
(TTeC ₃ -TTF)TCNQ									
Te1	13007(1)	2064(1)	11344(1)	5.9	C8	13140(24)	4690(16)	6840(28)	15.3
Te2	15039(1)	3224(1)	8396(1)	6.0	C9	12332(21)	5563(12)	5240(23)	11.3
S1	10667(3)	420(2)	7796(4)	4.5	CC1	4799(12)	-113(8)	11532(14)	3.9
S2	12170(3)	1285(2)	5582(4)	4.4	CC2	6088(11)	698(7)	11538(13)	3.4
C1	10584(11)	355(8)	5699(13)	4.0	CC3	6237(11)	796(7)	9933(13)	3.7
C2	12287(11)	1528(8)	8689(13)	3.9	CC4	7158(11)	1405(8)	13047(13)	3.9
C3	12984(11)	1933(8)	7700(14)	3.9	CC5	7049(13)	1321(9)	14641(15)	5.2
C4	10757(13)	2306(9)	10442(15)	5.4	CC6	8427(12)	2235(8)	13089(16)	5.0
C5	10373(14)	3231(9)	9215(16)	5.7	N1	6990(12)	1259(8)	15973(13)	6.9
C6	11408(16)	4302(11)	10058(20)	8.1	N2	9450(12)	2930(8)	13136(15)	7.2
C7	13756(22)	4335(13)	6176(24)	13.4					

a) Positional parameters ($\times 10^5$).

maximum deviation of only 0.033 Å for CC(1). The planar structure is commonly observed in many TCNQ complexes.

Figures 3(a) and 3(b) show the intermolecular overlap between the donor and the acceptor of p-(TSeC₂-TTF)TCNQ and n-(TSeC₂-TTF)TCNQ, respectively. In the case of p-(TSeC₂-TTF)TCNQ, a six-membered ring of TCNQ overlaps one of the two five-membered rings of TSeC₂-TTF. This overlapping manner is denoted as the p-mode. On the other hand, n-(TSeC₂-TTF)TCNQ has a disadvantageous donor-acceptor overlap with a smaller overlap between a six-membered ring of TCNQ and a five-membered ring of TSeC₂-TTF. This overlapping manner is denoted as the n-mode.

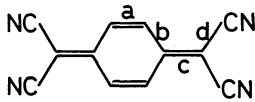
Figures 4(a) and 4(b) show the crystal structures of p-(TSeC₂-TTF)TCNQ and n-(TSeC₂-TTF)TCNQ, respectively. In both complexes, the donor and acceptor molecules alternately stack along the a-axis. The molecular short axis of the C₆S₄Se₄ molecular plane is nearly parallel to the c-axis.

The molecular structure of TTeC₃-TTF in the (TTeC₃-TTF)TCNQ complex is analogous to that of TSeC₂-TTF in n-(TSeC₂-TTF)TCNQ and the donor-acceptor

overlapping mode is analogous to that of p-(TSeC₂-TTF)TCNQ. The characteristic difference between (TTeC₃-TTF)TCNQ and the other complexes is that in the (TTeC₃-TTF)TCNQ complex the stacking axis is [101] which is different from the growing axis [100] of the crystal.

We have observed interchain atomic contacts in the (TxC₂-TTF)TCNQ complexes which are shorter than the sum of the van der Waals radii. n-(TSeC₂-TTF)TCNQ possesses a contact between the outer chalcogen atoms, while (TTeC₂-TTF)TCNQ possesses a contact between the outer chalcogen atom and the nitrogen atom. The shortest distances are 3.58 Å (Se(2)-Se(2) in n-(TSeC₂-TTF)TCNQ) and 3.28 Å (Te(2)-N(2) in (TTeC₂-TTF)TCNQ). In contrast, (TxC₃-TTF)TCNQ complexes do not possess any interchain atomic contacts due to a disturbance of the longer propyl groups elongated in the interchain direction.

Degree of Charge-Transfer. The degree of CT (γ) for the TCNQ complexes was estimated from the bond lengths of TCNQ by the procedure developed by Kistenmacher et al.²³⁾ Table 3 presents the calculated values of γ for the present TCNQ complexes.

Table 3. Bond Lengths of TCNQ and Degree of Charge-Transfer for (TxC_n-TTF)TCNQ


	a/Å	b ^{a)/Å}	c/Å	d ^{a)/Å}	c/(b+d)	γ	
(TTC ₂ -TTF)TCNQ	1.331(9)	1.439(8)	1.369(9)	1.429(8)	0.477	0.04	
(TTC ₃ -TTF)TCNQ	1.327(10)	1.443(10)	1.377(10)	1.433(11)	0.479	0.13	
(TSeC ₂ -TTF)TCNQ							
Plate	1.350(8)	1.436(8)	1.383(8)	1.430(8)	0.483	0.29	
Needle	1.343(11)	1.426(10)	1.397(11)	1.435(11)	0.488	0.50	
(TSeC ₃ -TTF)TCNQ	1.363(11)	1.434(9)	1.393(11)	1.435(10)	0.486	0.42	
(TTeC ₂ -TTF)TCNQ	1.340(6)	1.434(6)	1.386(6)	1.428(6)	0.484	0.33	
(TTeC ₃ -TTF)TCNQ	1.352(13)	1.426(17)	1.395(12)	1.404(18)	0.493	0.71	
TCNQ	1.346(3)	1.448(4)	1.374(3)	1.441(3)	0.476	0	Ref. 23
TCNQ ⁻	1.373(4)	1.423(4)	1.420(4)	1.416(4)	0.500	1	Ref. 23

a) The average value of the two equivalent bond lengths.

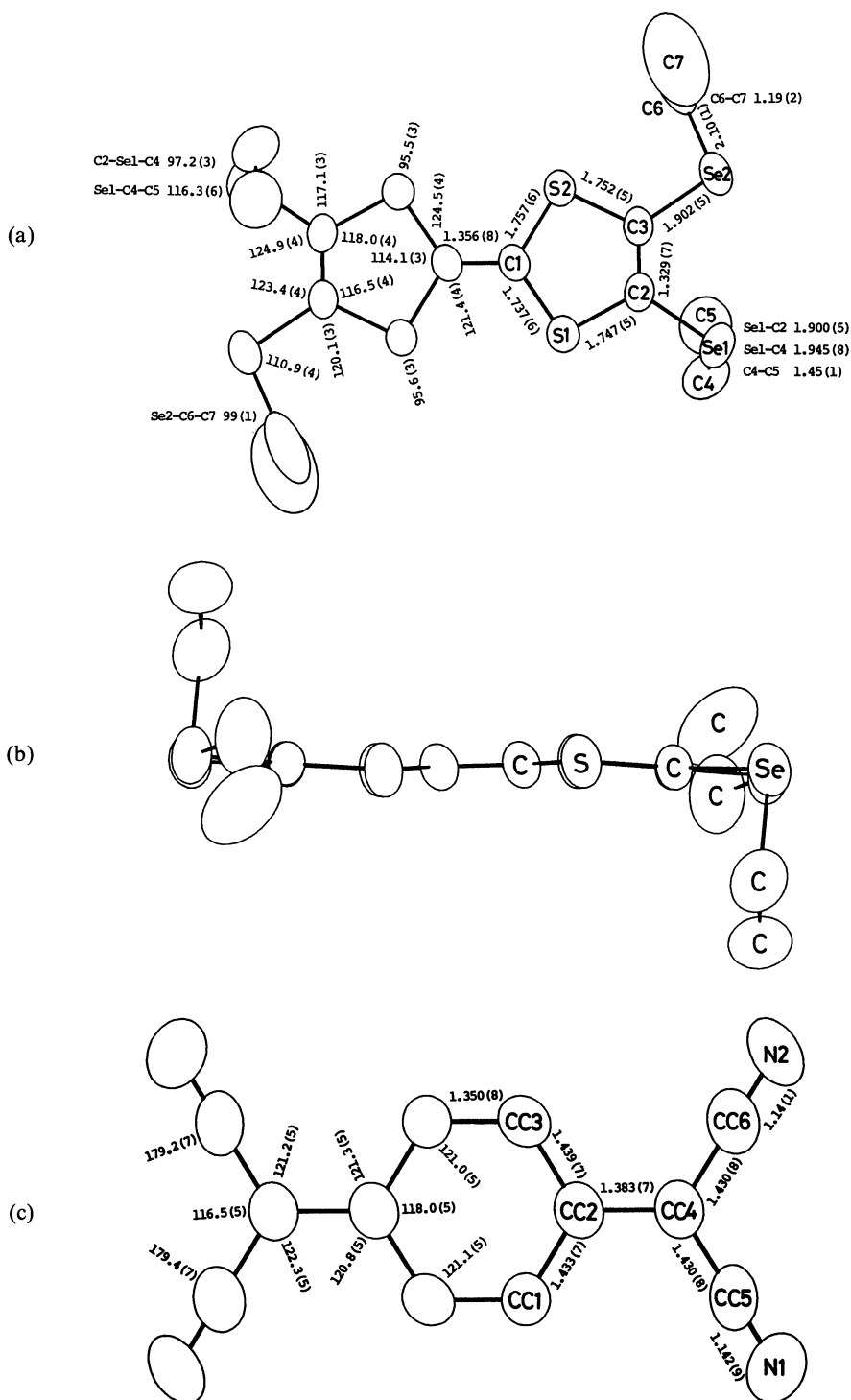


Fig. 1. Molecular structures and atomic numbering schemes of the donor (top view (a) and side view (b)) and the acceptor (c) of p-(TSeC₂-TTF)TCNQ.

are also listed in Table 4. The charge-transfer transition energy (E_{CT}) in a neutral complex with a mixed-stack can be expressed by the following equation:²⁵⁾

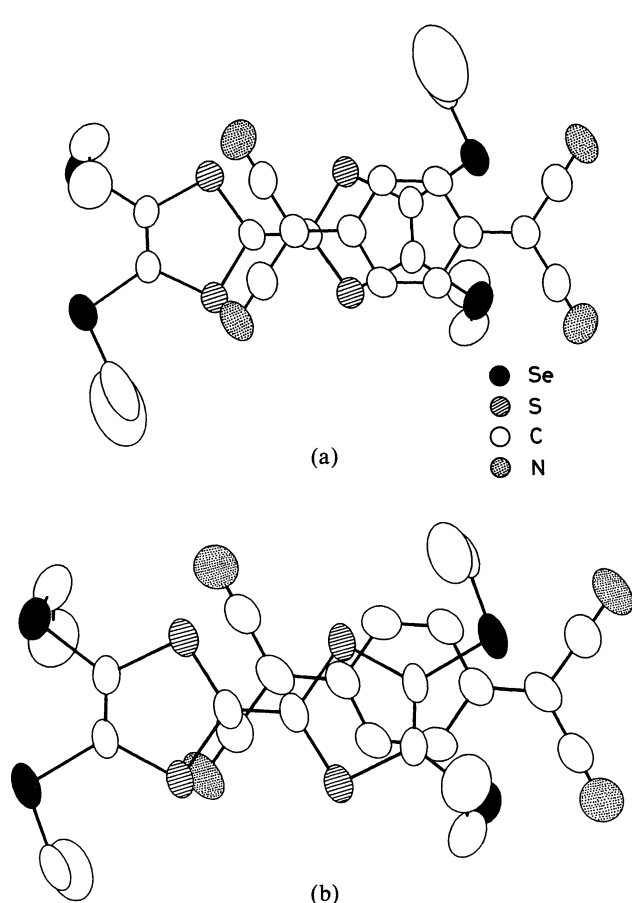
The electronic spectra in the KBr pellets showed the charge-transfer bands. These CT absorption energies

$$E_{CT} = I_p - E_A - E_M,$$

estimated values of γ . However, $\text{TTC}_n\text{-TTF}(n=2,3)\cdot\text{TCNQ}$, $\text{TSeC}_n\text{-TTF}(n=2,3)\cdot\text{TCNQ}$, and $\text{TTeC}_n\text{-TTF}(n=2,3)\cdot\text{TCNQ}$ had about the same CT absorption energies (6100—5200 cm^{-1} , 4700—4600 cm^{-1} , and 4200—3900 cm^{-1} , respectively). This fact suggested that γ of

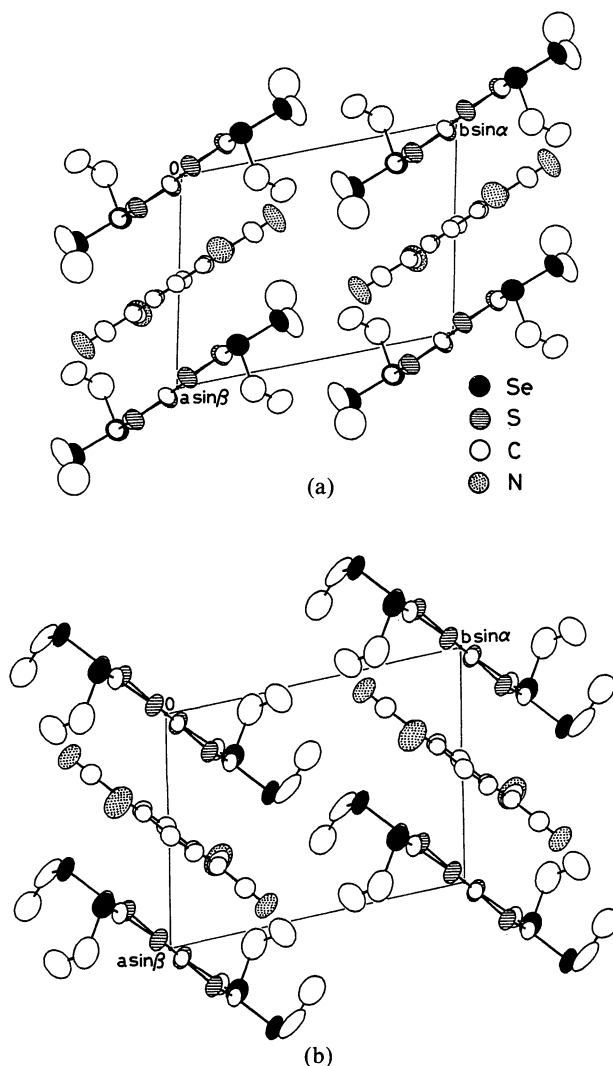
Table 4. Degree of Charge-Transfer (γ) Calculated by the IR Method, Charge-Transfer Absorption Energy (E_{CT}), and Electrical Properties of $(\text{TXC}_n\text{-TTF})\text{TCNQ}$

	$\nu_{\text{CN}}/\text{cm}^{-1}$	γ	$E_{\text{CT}}/\text{cm}^{-1}$	$\rho_{\text{RT}}/\Omega \text{ cm}$	E_a/eV
$(\text{TTC}_2\text{-TTF})\text{TCNQ}$	2214	0.30	6100	3.6×10^7	0.35
$(\text{TTC}_3\text{-TTF})\text{TCNQ}$	2214	0.30	5200	1.2×10^6	0.33
$(\text{TSeC}_2\text{-TTF})\text{TCNQ}$					
Plate	2212	0.34	4700	3.5×10^3	0.09
Needle	2216	0.25	4700	2.3×10^5	0.29
$(\text{TSeC}_3\text{-TTF})\text{TCNQ}$	2214	0.30	4600	2.2×10^6	0.39
$(\text{TTeC}_2\text{-TTF})\text{TCNQ}$	2206	0.48	4200	5.0	0.06
$(\text{TTeC}_3\text{-TTF})\text{TCNQ}$	2204	0.52	3900	7.5×10^3	0.18

Fig. 3. Overlapping modes between the donor and acceptor molecules; (a) $p\text{-(TSeC}_2\text{-TTF)TCNQ}$, (b) $n\text{-(TSeC}_2\text{-TTF)TCNQ}$.

$\text{TTC}_n\text{-TTF}(n=2,3) \cdot \text{TCNQ}$, $\text{TSeC}_n\text{-TTF}(n=2,3) \cdot \text{TCNQ}$, and $\text{TTeC}_n\text{-TTF}(n=2,3) \cdot \text{TCNQ}$ were in the ranges of 0.04–0.30, 0.25–0.50, and 0.33–0.71, respectively.

In the present system, γ increased in the order $\text{TTC}_n\text{-TTF}(n=2,3) \cdot \text{TCNQ} < \text{TSeC}_n\text{-TTF}(n=2,3) \cdot \text{TCNQ} < \text{TTeC}_n\text{-TTF}(n=2,3) \cdot \text{TCNQ}$. According to the cyclic voltammetry studies of $\text{TXC}_n\text{-TTF}$ ($\text{X}=\text{S}, \text{Se}, \text{Te}; n=1-18$),⁹⁾ the first redox potentials of $\text{TXC}_n\text{-TTF}$ compounds were independent of n and decreased in the order $\text{TTC}_n\text{-TTF} > \text{TSeC}_n\text{-TTF} > \text{TTeC}_n\text{-TTF}$. Thus, the tendency of the ionicity observed in the present system could be explained by the decrease of $(I_p - E_A)$.

Fig. 4. Crystal structures projected along the c -axis; (a) $p\text{-(TSeC}_2\text{-TTF)TCNQ}$, (b) $n\text{-(TSeC}_2\text{-TTF)TCNQ}$.

Electrical Conductivity. The electrical resistivity at room temperature (ρ_{RT}) and the activation energy (E_a) are given in Table 4. $(\text{TTeC}_2\text{-TTF})\text{TCNQ}$ showed a markedly low resistivity of $5 \Omega \text{ cm}$, which was smaller than the value (ca. $10^2 \Omega \text{ cm}$) reported by Aharon-Shalom et al.²¹⁾ The measurement by Aharon-Shalom et al. may have included a contact resistance. $p\text{-(TSeC}_2\text{-TTF)TCNQ}$ and $(\text{TTeC}_3\text{-TTF})\text{TCNQ}$ also showed

relatively low resistivities of 3.5×10^3 and $7.5 \times 10^3 \Omega \text{ cm}$, respectively. The other complexes showed comparatively high resistivities of 10^5 – $10^7 \Omega \text{ cm}$. The temperature dependence of the resistivities for all the complexes was simply semiconductive, which resulted from the alternate stacks of the donor and acceptor molecules in their crystal structures. (TTeC₂-TTF)-TCNQ, which had the lowest resistivity, had the lowest E_a (0.06 eV).

The electrical conductivity is universally expressed by a simple relation: $\sigma = ne\mu$. The carrier number n and the carrier mobility μ are believed to depend on γ and the magnitude of the molecular orbital overlap of the donor and the acceptor in the crystal, respectively. According to the band calculation by the extended Hückel method,²⁶⁾ the intermolecular overlap integrals between the highest occupied molecular orbital (HOMO) of TSeC₂-TTF and the lowest unoccupied molecular orbital (LUMO) of TCNQ along the stacking direction were -8.78×10^{-3} and 7.36×10^{-3} for p-(TSeC₂-TTF)TCNQ and n-(TSeC₂-TTF)TCNQ, respectively. The p-mode had an overlap integral larger than of the n-mode.

The high resistivities of (TTC₂-TTF)TCNQ and (TTC₃-TTF)TCNQ are easily understood in terms of the smaller γ values. n-(TSeC₂-TTF)TCNQ and (TSeC₃-TTF)TCNQ also showed high resistivities due to the n-mode overlap with a smaller overlap integral (as shown in Fig. 3(b)) in spite of having a larger γ than the S analogues.

The best planes for the C₆S₄X₄ (X=S, Se, Te) moieties of the donor and TCNQ were parallel to each other. The interplanar distances were 3.45, 3.44, 3.51, 3.49, 3.43, 3.57, and 3.47 Å for (TTC₂-TTF)TCNQ, (TTC₃-TTF)TCNQ, p-(TSeC₂-TTF)TCNQ, n-(TSeC₂-TTF)TCNQ, (TSeC₃-TTF)TCNQ, (TTeC₂-TTF)TCNQ, and (TTeC₃-TTF)TCNQ, respectively. These complexes had nearly the same interplanar spacings, which meant that the complexes including Se and Te atoms with larger van der Waals radii had stronger intermolecular interactions than the S analogues. The lower resistivities of p-(TSeC₂-TTF)TCNQ, (TTeC₂-TTF)TCNQ, and (TTeC₃-TTF)TCNQ compared with the S analogues are qualitatively explained in terms of the difference of the van der Waals radii of the chalcogen atoms. (TTeC₂-TTF)TCNQ had the lowest resistivity among the present complexes, owing to the p-mode overlap with a larger overlap integral (as shown in Fig. 3(a)) and the effective γ .

(TTeC₃-TTF)TCNQ possessed the p-mode overlap shown in Fig. 3(a) and the highest γ . However, (TTeC₃-TTF)TCNQ showed a higher resistivity than (TTeC₂-TTF)TCNQ, because of a mismatch between the measuring direction of the conductivity and the stacking direction of the donor and acceptor molecules. If we can measure along the stacking axis, a lower resistivity of (TTeC₃-TTF)TCNQ is expected to be observed.

Finally, we compared the crystal structures and the

electrical properties of the TXC₁-TTF (X=S, Se, Te)-TCNQ complexes.^{9,14-16)} The structural and physical properties of TXC_{*n*}-TTF (X=S, Se, Te; *n*=1,2,3)-TCNQ complexes are presented in Table 5. The molecular structure of the donor and the donor(D)-acceptor(A) overlapping mode in TXC₁-TTF (X=S, Se, Te)-TCNQ were analogous to those of p-(TSeC₂-TTF)TCNQ. (TTeC₁-TTF)TCNQ made simple DA type stacks, similar to TXC_{*n*}-TTF (X=S, Se, Te; *n*=2,3)-TCNQ. In contrast, (TTC₁-TTF)TCNQ and (TSeC₁-TTF)TCNQ formed DDAA mixed-stacks, and (TTC₁-TTF)₂TCNQ formed a DDA mixed-stack.

(TTC₁-TTF)TCNQ and (TSeC₁-TTF)TCNQ had interchain atomic contacts between the outer chalcogen atom and the nitrogen atom, similar to (TTeC₂-TTF)TCNQ. In particular, (TTeC₁-TTF)TCNQ had a unique crystal structure with three-dimensional intermolecular interactions through two kinds of DA stacks along the [110] and [$\bar{1}\bar{1}0$] direction and strong interchain Te-N contacts. These chalcogen-N interactions modulated the CN stretching vibration frequency and caused an overestimation of γ by the IR method for (TXC₁-TTF)TCNQ.

Judging from the value of γ calculated by the X-ray method and E_{CT} , (TTC₁-TTF)TCNQ, (TTC₁-TTF)₂TCNQ, and (TSeC₁-TTF)TCNQ were in the neutral CT state, similar to TTC_{*n*}-TTF (*n*=2,3)-TCNQ. It was difficult to determine the ionicity of (TTeC₁-TTF)TCNQ by the IR and X-ray methods.

Summary

TXC_{*n*}-TTF (X=S, Se, Te; *n*=2,3) formed semiconductive 1:1 CT complexes with TCNQ, in which donor and acceptor molecules alternately stacked with a uniform spacing. This situation was in contrast to (TXC₁-TTF)-TCNQ complexes with a variety of stoichiometries and donor-acceptor stacks. It was of interest that (TSeC₂-TTF)TCNQ crystallized in plates and needles. These two phases had different crystal structures and showed different electrical properties. The crystal structures of the other complexes were isomorphous to either p-(TSeC₂-TTF)TCNQ or n-(TSeC₂-TTF)TCNQ.

The ionicity of TXC_{*n*}-TTF (X=Se, Te; *n*=2,3)-TCNQ was at the boundary between the neutral (N) and ionic (I) states. These complexes may exhibit an N-I phase transition induced by temperature and/or pressure.

(TXC₁-TTF)TCNQ and (TXC₂-TTF)TCNQ had two- or three-dimensional networks in the crystals through intrachain and interchain atomic contacts less than the van der Waals distance. On the other hand, (TXC₃-TTF)TCNQ was one-dimensional. TXC_{*n*}-TTF (*n*≥4) did not form CT complexes with TCNQ. The reason was speculated to be a decrease of lattice energy by further weakened interchain interactions, in addition to a size mismatch between the donor and TCNQ molecules.

Table 5. Summary of Structural and Physical Properties of (TxC_n-TTF)-TCNQ Complexes

<i>n</i>	X=T (Sulfur) ^{a)}					X=Se ^{a)}			X=Te ^{a)}
1	D:A	1:1		2:1		1:1			1:1
	Stacking	DDAA		DDA		DDAA			DA
	Spacing	Non-uniform		Non-uniform		Non-uniform			Uniform
	/Å	D··D	A··A	D··A	D··D	D··A	D··D	A··A	D··A
		3.48	3.41	3.58	3.51	3.60	3.51	3.38	3.28
	Molecular structure	p-Form ^{b)}		p-Form		p-Form			p-Form
	Mode of DA overlap	p-Mode ^{b)}		p-Mode		p-Mode			p-Mode
	γ (X-ray)	0.04		0.25		0.29			>1
	γ (IR)	0.57		0.43		0.61			>1
	<i>E</i> _{CT} /cm ⁻¹	6000		5100		6000			4800
2	<i>ρ</i> _{RT} /Ω cm	3.8×10 ⁵		5.5×10 ⁴		1.5×10 ⁵			1.0×10 ²
	<i>E</i> _a /eV	0.30		0.17		0.35			0.11
	Melting point/°C	111—112		105		131—132			312—315
3	D:A	1:1				1:1			1:1
	Stacking	DA				DA			DA
	Spacing	Uniform				Uniform			Uniform
	/Å	3.45				3.51			3.57
	Molecular structure	n-Form ^{b)}				p-Form			p-Form
	Mode of DA overlap	n-Mode ^{b)}				p-Mode			p-Mode
	γ (X-ray)	0.04				0.29			0.33
	γ (IR)	0.30				0.34			0.48
	<i>E</i> _{CT} /cm ⁻¹	6100				4700			4200
	<i>ρ</i> _{RT} /Ω cm	3.6×10 ⁷				3.5×10 ³			5.0 (~10 ^{2c)})
4	<i>E</i> _a /eV	0.35				0.09			0.06
	Melting point/°C	108—109				108—109			151—154
5	D:A	1:1				1:1			1:1
	Stacking	DA				DA			DA
	Spacing	Uniform				Uniform			Uniform
	/Å	3.44				3.43			3.47
	Molecular structure	p-Form				n-Form			n-Form
	Mode of DA overlap	p-Mode				n-Mode			p-Mode
	γ (X-ray)	0.13				0.42			0.71
	γ (IR)	0.30				0.30			0.52
	<i>E</i> _{CT} /cm ⁻¹	5200				4600			3900
	<i>ρ</i> _{RT} /Ω cm	1.2×10 ⁶				2.2×10 ⁶			7.5×10 ³
6	<i>E</i> _a /eV	0.33				0.39			0.18
	Melting point/°C	95—96				100—101			87—89

a) The first redox potential (*E*_{1/2}) vs. SCE 0.1 M TBA·BF₄/CH₂ClCH₂Cl, Pt electrode: 0.64 V (TTC_n-TTF), 0.58 V (TSeC_n-TTF), 0.51 V (TTeC_n-TTF). b) The abbreviation is described in the text. c) The value reported by Aharon-Shalom et al. (Ref. 21).

The authors wish to thank Dr. Susumu Matsuzaki of Kumamoto University for his measurements of the IR spectra. They are also grateful to Professor Kazuhiro Nakasuji of the Institute for Molecular Science for his helpful discussions.

References

- 1) H. Inokuchi, G. Saito, P. Wu, K. Seki, T. B. Tang, T. Mori, K. Imaeda, T. Enoki, Y. Higuchi, K. Inaka, and N. Yasuoka, *Chem. Lett.*, **1986**, 1263.
- 2) K. Seki, T. B. Tang, T. Mori, P. Wu, G. Saito, and H. Inokuchi, *J. Chem. Soc., Faraday Trans. 2*, **82**, 1067 (1986).
- 3) K. Imaeda, T. Enoki, Z. Shi, P. Wu, N. Okada, H. Yamochi, G. Saito, and H. Inokuchi, *Bull. Chem. Soc. Jpn.*, **60**, 3163 (1987).
- 4) Z. Shi, T. Enoki, K. Imaeda, K. Seki, P. Wu, H.

Inokuchi, and G. Saito, *J. Phys. Chem.*, **92**, 5044 (1988).

- 5) H. Inokuchi, K. Imaeda, T. Enoki, T. Mori, Y. Maruyama, G. Saito, N. Okada, H. Yamochi, K. Seki, Y. Higuchi, and N. Yasuoka, *Nature*, **329**, 39 (1987).
- 6) G. Saito, *Physica B, Amsterdam*, **143**, 296 (1986).
- 7) N. Okada, H. Yamochi, F. Shinozaki, K. Oshima, and G. Saito, *Chem. Lett.*, **1986**, 1861.
- 8) H. Yamochi, N. Iwasawa, H. Urayama, and G. Saito, *Chem. Lett.*, **1987**, 2265.
- 9) N. Iwasawa, Ph. D. Thesis, The University of Tokyo, Tokyo, Japan, 1987.
- 10) P. Wu, G. Saito, K. Imaeda, Z. Shi, T. Mori, T. Enoki, and H. Inokuchi, *Chem. Lett.*, **1986**, 441.
- 11) P. Wu, T. Mori, T. Enoki, K. Imaeda, G. Saito, and H. Inokuchi, *Bull. Chem. Soc. Jpn.*, **59**, 127 (1986).
- 12) G. Saito, H. Kumagai, C. Katayama, C. Tanaka, J. Tanaka, P. Wu, T. Mori, K. Imaeda, T. Enoki, H. Inokuchi, Y.

Higuchi, and N. Yasuoka, *Isr. J. Chem.*, **27**, 319 (1986).

13) K. Imaeda, T. Enoki, T. Mori, P. Wu, M. Kobayashi, H. Inokuchi, and G. Saito, *Synth. Met.*, **19**, 721 (1987).

14) T. Mori, P. Wu, K. Imaeda, T. Enoki, H. Inokuchi, and G. Saito, *Synth. Met.*, **19**, 545 (1987).

15) N. Iwasawa, H. Urayama, H. Yamochi, G. Saito, K. Imaeda, T. Mori, Y. Maruyama, H. Inokuchi, T. Enoki, Y. Higuchi, and N. Yasuoka, *Synth. Met.*, **27**, B463 (1988).

16) N. Iwasawa, F. Shinozaki, G. Saito, K. Oshima, T. Mori, and H. Inokuchi, *Chem. Lett.*, **1988**, 215.

17) P. Main, S. E. Hull, L. Lessinger, G. Germain, J. P. Declercq, and M. M. Woolfson, MULTAN 78, Univ. of York, England and Louvain, Belgium (1978).

18) "International Tables for X-Ray Crystallography," Kynoch Press, Birmingham (1974), Vol. IV.

19) T. Sakurai and K. Kobayashi, *Rep. Inst. Phys. Chem. Res.*, **55**, 69 (1978).

20) Tables of atomic parameters of H-atoms, anisotropic thermal parameters, the F_o-F_c lists, bond distances, bond

angles, and equations of the planes are deposited as Document No. 9200 at the Office of the Editor of Bull. Chem. Soc. Jpn.

21) E. Aharon-Shalom, J. Y. Becker, J. Bernstein, S. Bittner, and S. Shaik, *Synth. Met.*, **11**, 213 (1985). Their final R value is 0.051 for 2291 reflections, while $R=0.038$ for 4074 reflections in our work. Thus, we report crystallographic data as a well-refined structure for (TTeC₂-TTF)TCNQ.

22) P. Wang, T. Mori, C. Nakano, Y. Maruyama, H. Inokuchi, N. Iwasawa, H. Yamochi, H. Urayama, and G. Saito, *Bull. Chem. Soc. Jpn.*, **61**, 3455 (1988).

23) T. J. Kistenmacher, T. J. Emge, A. N. Bloch, and D. O. Cowan, *Acta Crystallogr., Sect. B*, **38**, 1193 (1982).

24) J. S. Chappell, A. N. Bloch, W. A. Bryden, M. Maxfield, T. O. Poehler, and D. O. Cowan, *J. Am. Chem. Soc.*, **103**, 2442 (1981).

25) J. B. Torrance, J. E. Vazquez, J. J. Mayerle, and V. Y. Lee, *Phys. Rev. Lett.*, **46**, 253 (1981).

26) T. Mori, A. Kobayashi, Y. Sasaki, H. Kobayashi, G. Saito, and H. Inokuchi, *Bull. Chem. Soc. Jpn.*, **57**, 627 (1984).
